Application of 2-D deformable-layer tomostatics in western China

Peiming Li, Zhihui Yan, and Yongqing He, BGP*
Hua-wei Zhou, Hui Liu, Fan Jiang, Texas Tech University

Summary

We applied a deformable-layer tomography (DLT) method to the tomostatics study. The advantage of the DLT is to directly invert for the geometry of velocity interfaces. In contrast, conventional tomostatics invert for the velocity values of a fixed-in-space framework of grids or cells, and the thickness of the layers can only be interpreted after inversion. The DLT approach allows an inversion for both the thickness and velocity of the weathering zone and basement layers. The method is tested with a field data from Chaidam Basin, western China. The result indicates that the DLT yielded a geologically reasonable near-surface velocity model, and the corresponding stack section shows significant improvement in comparison with the sections from commercial tomostatics software.

Introduction

Tomostatics is a technique to determine the near-surface static contribution to reflection seismic data based on velocity models derived from traveltime tomography (e.g., De Amorim *et al*., 1987; Docherty, 1992; Zhu *et al*., 1992; Rajasekaran and McMechan, 1996; Al-Rufaii et al., 2001; Chang et al., 2002). However, the tomography methods of all commercial tomostatics software that we have seen so far invert for velocity values of a framework of nodes or cells that are fixed in the model spaces. Some problems of the cell-based tomography in model dissection have been discussed by Yan et al. (2007).

In the presence of strong fluctuation of the surface topography and the subsurface velocity interfaces or in the presence of layer pinchouts, the fixed-in-space rectangular grids or cells will not be able to properly describe the geologic or velocity models. The topography and the subsurface interfaces after model dissecting become stair-stepped (see Figure 1, Upper panel), resulting in large error with respect to the actual interfaces. The use of too small grid sizes may lead to low ray coverage and too many inversion unknowns, resulting in poor tomographic solutions.

Here we adopted the deformable-layer tomography (DLT) method (Zhou, 2006) to solve the tomostatics problem. The thickness-varying layered models of DLT (Figure 1, Lower panel) are suitable for tomostatics applications. The most beneficial point is that DLT directly inverts for the geometry of model interfaces and layer velocities. The detail of our method and result from a field data test are shown in this paper.

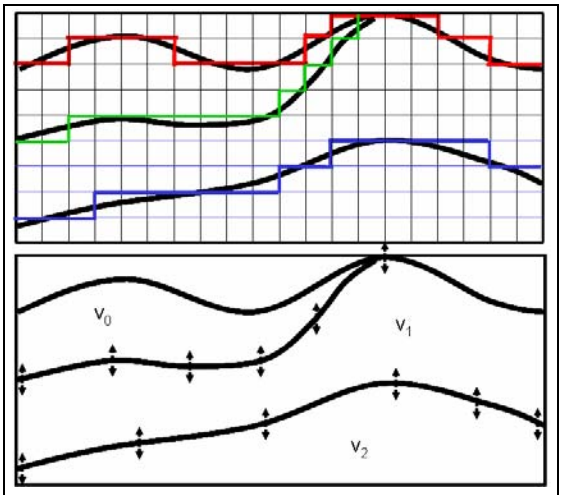

Figure 1: (Upper) Cell tomography dissects the depth-vary interfaces into blocky boundaries in different colors. (Lower) Deformable-layer tomography allows a direct inversion for the geometry of velocity interfaces.

Methodology

The DLT method is motivated by two observations. First, most near-surface geologic features, such as the weathering zone and stratigraphic beddings, resemble thickness-varying layers and pinch-outs rather than regularly spaced blocky cells. Second, the range of velocity values is known a priori to velocity model building, based on surface geology, well logs, and previous seismic studies. One can, for example, estimates average velocities from the traveltime-distance plots. A much meaningful goal then is to find the spatial position of particular velocity values, such as that for the weathering layer, water, sands, limestone, salt, etc. Therefore, it makes more sense if we can determine the spatial position of major velocity contours, rather than determining velocity as a function of space. The former approach may allow a determination of the geometry of major velocity interfaces with a minimum number of model variables adapting to the geologic configuration.

A 2D synthetic example of deformable-layer tomostatics is shown in Figures 2 and 3. The true velocity model is 10 km in length and 0.7 km in depth, with velocities ranging from 0.8 km/s to 3 km/s. The data consists of 420 first-arrival turning rays from 20 shots to 21 receivers placed on a

variable topography. Started from an initial reference model (Figure 2c) of equal-thickness layers excepting the top layer, the solutions of the DLT iterations are shown in Figure 2d to 2f, with the true interface geometry indicated by dotted curves. The traveltime data contain a small amount of Gaussian noise, with a standard deviation of 20 ms, which is approximately 1% of the average traveltime. Here DLT attempts to solve for both the interface geometry and the layer velocities.

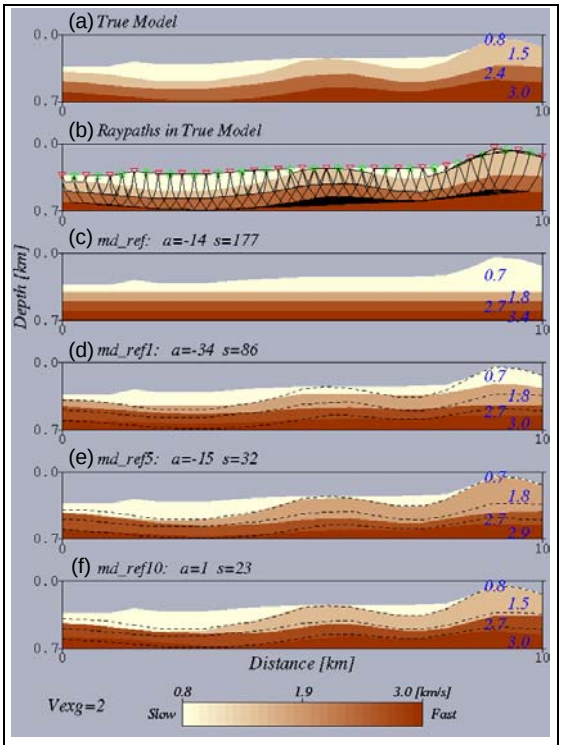

Figure 2: 2D synthetic tests of Deformable-layer tomography (DLT) using first arrivals. (a) The true velocity model. (b) First-arrival raypaths. (c) The initial reference model. (d) Iteration 1 solution. (e) Iteration 5 solution. (f) Iteration 10 solution, taken as the final DLT model. The blue-colored values shown near the right end of the models are layer velocities in km/s. The dashed curves in (d) to (f) denote the position of true model interfaces. There is a 2:1 vertical exaggeration.

The 10th iteration DLT solution in Figure 2f is taken as the final DLT model, which is a very good representation of the true velocity model for both interface geometry and interval velocities. From the top layer downwards, the differences in layer velocities between the true model and the initial reference model are 0.1, -0.3, -0.3, and -0.4 km/s, respectively. Three out of the four velocity differences are reduced to less than 0.05 km/s in the final DLT model. Only the third layer of the final model has a layer velocity of 2.7 km/s that differs from that of the true model of 2.4 km/s. Notice that this third layer in the final model is generally deeper than that of the true model, reflecting its anomalously high velocity. Several pinchouts in the top layer are well resolved by the DLT. The traveltime residuals of the final DLT model have a mean of 1.26 ms and a standard deviation of 23.3 ms for the dataset that included Gaussian noise with a standard deviation of 20 ms.

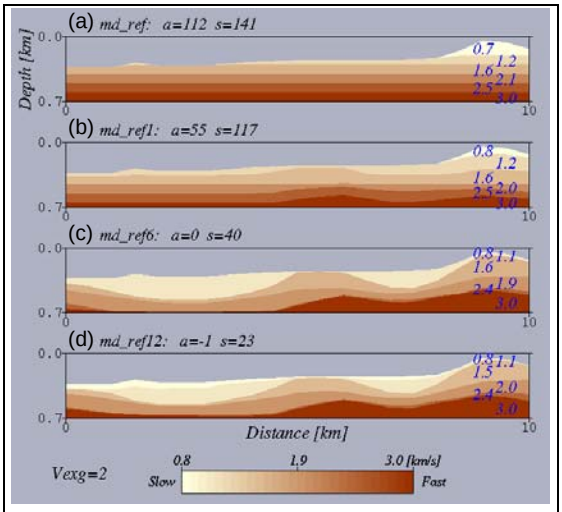

Figure 3: 2D synthetic tests of Deformable-layer tomography (DLT) with the four-layer model in Fig. 3a as the true velocity model but using six layers in the inversion. (a) The initial reference model. (b) Iteration 1 solution. (c) Iteration 6 solution. (d) Iteration 12 solution, taken as the final DLT model for this case. The blue-colored values shown near the right end of the models are layer velocities in km/s. There is a 2:1 vertical exaggeration.

Figure 3 shows the results of a further synthetic test with the same noise-added data from the four-layer true model in Figure 3a, but with six-layer models in the tomographic inversion. The iteration 12 solution (Figure 3d) is taken as the final DLT model. The six-layer solutions in Figure 3 clearly attempt to match the four-layer true model in Figure 2a. The layer velocities and interface geometry of the six-layer final solution in Figure 3d are located reasonably close to the right values of the true four-layer model. The nearly identical data fitness levels of Figures 2f and 3d demonstrate the nonuniqueness of the tomographic solutions with the same dataset.

Field data case

The 2D seismic line for our field test is from the Haitugou area in southeastern Chaidam Basin, which has the most complex near-surface conditions for seismic prospecting in China. The area is covered by sand dunes and gravels. In

the sand dunes areas the near-surface weathering zone has three layers: The top loose sand layer with a velocity of 500-600 m/s; The middle sedimentary sand layer with a velocity of 800-1100 m/s; and the bottom black gravel layer with a velocity greater than 1700 m/s. The total thickness of the weathering zone is 30-200 m. The gravel areas have two layers: The top sedimentary sand layer and the bottom black gravel layer. The low velocity of the sedimentary sand layer is 400-500 m/s, the sub-weathering velocity is 800-1200 m/s. The extremely large variation in the near-surface velocities makes the static correction problem a very serious one.

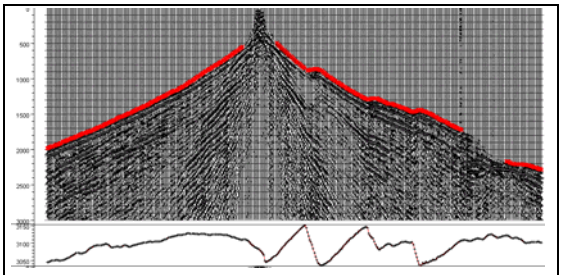

Figure 4: A typical shot gather from the field dataset.

The data are very noisy with strong ground rolls (Figure 4) and reflections are hardly visible. The survey is carried out with roll-in and roll-out geometry, it produces 399 shots totally. The largest trace number for each shot is 480. The shot interval is 60 m and receiver interval is 30 m. The shot to receiver offsets is limited to be less than 2000 m for testing different static correction methods.

Figure 5 shows the velocity models produced from the iterative DLT processing. The initial DLT velocity model has seven layers. The initially assigned velocities and the corresponding six internal interfaces are shown in Figure 5a. The velocity ranges from 600 m/s to 4000 m/s. The final DLT model (Figure 5d) shows the base of the low-velocity zone as a smooth interface above the layer with 2700 m/s in velocity. Overall the DLT solutions converge nicely to the final model that is geologically reasonable.

We have calculated the first break refraction static corrections as well as tomostatics corrections using two types of commercial software. For the two commercial tomostatics software, the cell sizes are 60 m in horizontal and 5 m in depth. Both the initial velocity model of them are gradient models, the gradient comes from the near-surface investigation. We take the 10th iteration result as the final model.

Figure 6 compares the stack section based on the DLT model (Figure 5d) with stacks from two commercial tomostatics software as well as first-break refraction statics. For all methods compared, the final datum is at 3150 m in elevation, and the replacement velocity is 3000 m/s.

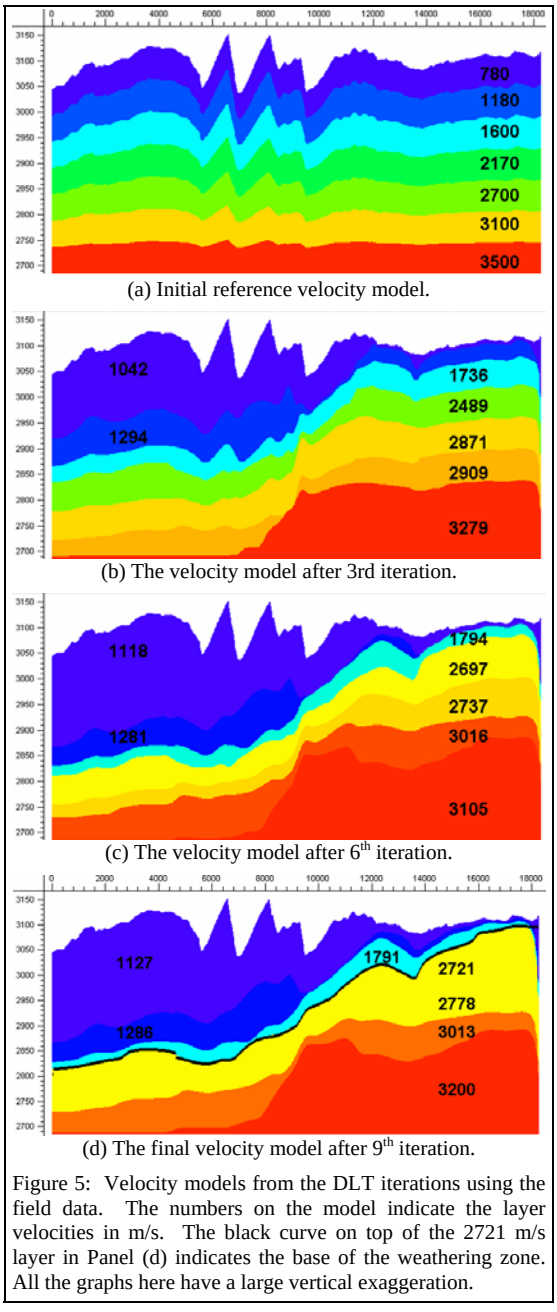

(a) Initial reference velocity model.

(b) The velocity model after 3rd iteration.

(c) The velocity model after 6th iteration.

(d) The final velocity model after 9th iteration.

Figure 5: Velocity models from the DLT iterations using the field data. The numbers on the model indicate the layer velocities in m/s. The black curve on top of the 2721 m/s layer in Panel (d) indicates the base of the weathering zone. All the graphs here have a large vertical exaggeration.

While it is nontrivial to exam the detail of stack sections, we evaluated the continuity of possible reflectors across the sections to assess the effectiveness of the four methods. To

help facilitate the analysis, three dashed ellipses in color are added to Figure 6. In the orange-colored ellipse in the upper-right corner of each panel, the DLT section has clearly better reflector continuity than the other three sections. Because that the effect of near-surface statics is at its maximum at the shallowest depth, the better result of the DLT in comparison with the other three methods is significant here. In the middle ellipse in green color, though all four results are comparable, the DLT and the refraction statics sections have more reflector continuity than the two commercial tomo-statics softwares. In the deepest ellipse in yellow color, the DLT section is somewhat better than the refraction statics section, and these two sections are significantly better than the sections from both commercial software.

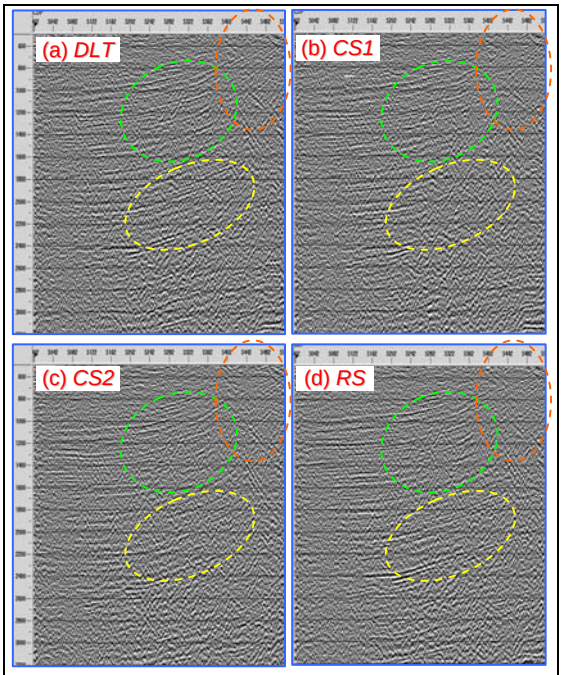

Figure 6: Comparison of stack sections from four different methods. (a) Deformable-layer tomography (DLT); (b) Commercial tomostatics software one (CS1); (c) Commercial tomostatics software two (CS2); (d) First-break refraction statics (RS). Three dashed ellipses in color are added to enhance the comparative analysis.

Discussion and conclusions

We have adopted the deformable-layer tomography (DLT) to the tomostatics problems because that DLT is capable to directly invert for the thickness variation of the weathering zone. This is advantageous than the existing commercial tomostatics software that invert for velocity values of a fixed-in-space framework of grids or cells. One reason for the advantage of DLT is that the velocity of the weathering zone and basement can be well estimated a priori to tomographic inversion, so the tomography effort shall focus on determine the geometry of the interface(s) between the main velocity layers. Another argument for DLT is that the number of inversion unknowns in the DLT is often smaller than that of the grid or cell tomography.

In conclusion, we have shown using field data in a complex land area that deformable-layer tomostatics resulted in a geologically reasonable near-surface velocity model, and the corresponding stack section indicates significant improvement in the continuity of reflection in comparison with the results from some current tomostatics methods.

Acknowledgements

We would like to thank Mrs. Yanjuan Wang for processing the seismic data, Mr. Yunfei Zu and Zheyuan Feng for calculating the static corrections with other softwares.

EDITED REFERENCES

Note: This reference list is a copy-edited version of the reference list submitted by the author. Reference lists for the 2008 SEG Technical Program Expanded Abstracts have been copy edited so that references provided with the online metadata for each paper will achieve a high degree of linking to cited sources that appear on the Web.

REFERENCES

Al-Rufaii, K., H. Zhou, and L. Lu, 2001, Tomographic velocity analysis in complex areas: 71st Annual International Meeting, SEG, Expanded Abstracts, 748–751.

Chang, X., Y. Liu, H. Wang, F. Li, and J. Chen, 2002, 3D tomographic static correction: Geophysics, **67**, 1275–1285.

De Amorim, W. N., P. Hubrail, and M. Tygel, 1987, Computing field statics with the help of seismic tomography: Geophysical Prospecting, **35**, 907–919.

Docherty, P., 1992, Solving for the thickness and velocity of the weathering layer using 2D refraction tomography: Geophysics, **57**, 1307–1318.

Rajasekaran, S., and G. A. McMechan, 1996, Tomographic estimation of the spatial distribution of statics: Geophysics, **61**, 1198–1208.

Yan, Z., P. Li, Q. Ma, Z. Feng, and X. Yang, 2007, Tomographic static corrections with vertically parallel irregular grids: Presented at the 77th Annual International Meeting, SEG.

Zhou, H., 2006, Multiscale deformable-layer tomography: Geophysics, **71**, R11–R19.

Zhu, X., D. P. Xista, and B. G. Angstman, 1992, Tomostatics: Turning-ray tomography + static corrections: The Leading Edge, **11**, 15–23.